Fingerprint image matching by minimization of a thin-plate energy using a two-step algorithm with auxiliary variables

Andrés Almansa

CMLA   Fac. de Ingeniería

ENS Cachan   Univ. de la República

94235 Cachan, France   11300 Montevideo, Uruguay

almansa@ieee.org

Laurent Cohen

CEREMADE

Université Paris Dauphine

75775 Paris, France

Laurent.Cohen@ceremade.dauphine.fr

Abstract

A common approach in fingerprint matching algorithms consists of minimizing a similarity measure between feature vectors of both images, over a set of linear transformations of one image to the other. In this work we propose the thin-plate spline as a more accurate model for the geometric transformations that arise in fingerprint images. In addition we show how such a model can be integrated into a matching algorithm by means of a two-step iterative minimization with auxiliary variables. Such a method allows to correct many of the false pairings of minutiae commonly found by matching algorithms based on linear transforms.

1. Introduction

Forensic experts [10, 7, 6, 9] usually look for a sufficient number of matching *minutiae* (*i.e.* branching points in the ridge structure of a fingerprint) in order to determine whether two fingerprint images correspond to the same person. Automatic matching algorithms roughly follow the same procedure, according to the dominant approaches reported in the literature [3, 14, 4, 18, 13, 11, 12]. The main difficulties for automating this task are still related to three aspects:

1. Fingerprint images are usually very *noisy*, which makes the *minutiae detection* task very difficult. Recent reports [17, 1] on the performance of minutia detection algorithms show a false negative rate ranging between 2% and 35% and a false positive rate ranging between 4% and 20%.

2. Hence *matching algorithms* have to deal with *partial* (due to false negatives) and *uncertain* (due to false pos-

itives) information. In addition the correspondence between minutia points in both images is not known.

3. Finally, the main difficulty concerns *the geometric distortion* between several images of the same fingerprint. This distortion is not necessarily linear, since the skin can be deformed in a more or less *elastic* manner.

Despite the importance of this last observation most classical techniques for fingerprint matching [3, 14, 18] are based on a rigid deformation model. In fact, the most common approach for obtaining a similarity measure between two fingerprints, consists in defining a suitable distance measure between two sets of minutiae, and then minimizing this distance over all possible rigid transformations and possibly certain rescalings.[1] Only recently [13, 11] did we know of certain attempts to consider fingerprint matching algorithms which rely on a non-rigid deformation model. However, these algorithms use an elastic deformation model only implicitly, since the non-rigid part of the deformation is found by a learning algorithm which imposes certain smoothness to the warping function.

Here we deal with the deformation model explicity and show the validity of a thin-plate energy as a model of the kind of deformations that are present in fingerprint images (section 2). We also show how such a model can be used to automatically detect point correspondences more accurately, when compared to rigid transformations (section 4). Finally we present an algorithm to decompose the possibly non-convex minimization into a series of easy-to-solve quadratic minimization problems (section 5), and we give several directions to further improve the proposed method (section 6).

---

[1]Alternatively, certain authors considered rotation-, scale-, and/or translation invariant distance measures between two sets of minutiae.

2. Elastic matching with known point-correspondences.

In order to validate the deformation model we shall propose, let us first consider a simplified matching problem, where we assume that we are given complete and reliable minutiae information. Consider the pair of fingerprint images shown in figures 1(a) and 1(b). They both correspond to the same finger of the same person. A forensic expert has marked the reliable minutiae in both images, as well as the correspondences between these points whenever possible. The images show a set of 40 corresponding minutiae that were visible in both images.

Let's denote by (p_i, p_i'), $i = 1, \dots, N = 40$ the pairs of corresponding minutiae. A valid deformation model should reconstruct a plausible deformation $f : \Omega \subseteq \mathbb{R}^2 \to \mathbb{R}^2$ which interpolates the point correspondences (p_i, p_i'), i.e.

$$f(p_i) = p_i' \quad \forall i = 1, \dots, N \tag{1}$$

In our case we used the thin-plate spline model [16, 5, 2], i.e., the interpolant $f = \binom{f_x}{f_y}$ which minimizes the thin-plate spline deformation energy:

$$E_{TPS}(f) = \frac{1}{2} \int_\Omega (R(f_x) + R(f_y)) \tag{2}$$

$$R(f) = \left(\frac{\partial^2 f}{\partial x^2}\right)^2 + 2\left(\frac{\partial^2 f}{\partial x \partial y}\right)^2 + \left(\frac{\partial^2 f}{\partial y^2}\right)^2 \tag{3}$$

The minimizer of equation (2) under the interpolation restriction (1) can be written in terms of the fundamental solution $U(x, y) = \tilde{U}(x^2 + y^2) = \tilde{U}(r^2) = r^2 \log(r^2)$ of the biharmonic equation $\Delta^2 U = \delta_{(0,0)}$ as:

$$f(x, y) = \mathbf{A} \begin{pmatrix} 1 \\ x \\ y \end{pmatrix} + \mathbf{W}\mathbf{U} \tag{4}$$

where $\mathbf{A} = \binom{\mathbf{A}_x}{\mathbf{A}_y}$ and $\mathbf{W} = \binom{\mathbf{W}_x}{\mathbf{W}_y}$ are 2×3 and $2 \times N$ coefficient matrices, and $\mathbf{U} = (U_1, \dots, U_N)$ is an $N \times 1$ column vector containing the values $U_i = U(\binom{x}{y} - \binom{x_i}{y_i})$ of the fundamental solution translated to each data point point $p_i = \binom{x_i}{y_i}$ in the first image. The coefficients $\mathbf{A}, \mathbf{W}$ for the interpolating minimizer are calculated by solving the linear system of equations:

$$\begin{aligned} \mathbf{KW}^T + \mathbf{PA}^T &= \mathbf{V}^T \\ \mathbf{P}^T\mathbf{W}^T &= 0 \end{aligned} \tag{5}$$

where the matrices $\mathbf{K}$, $\mathbf{P}$ and $\mathbf{V}$ are defined as:

$$K_{ij} = \begin{cases} U(p_i - p_j), & \text{if } i \neq j \\ 0, & \text{if } i = j \end{cases}, \tag{6}$$

$$\mathbf{P} = \begin{pmatrix} 1 & x_1 & y_1 \\ 1 & x_2 & y_2 \\ \vdots & \vdots & \vdots \\ 1 & x_N & y_N \end{pmatrix}, \tag{7}$$

$$\mathbf{V} = \begin{pmatrix} x_1' & x_2' & \cdots & x_N' \\ y_1' & y_2' & \cdots & y_N' \end{pmatrix}, \tag{8}$$

where (x_i, y_i) are the xy coordinates of the minutia point p_i, and (x_i', y_i') are the coordinates of the corresponding point p_i' in image 2. Finally the deformation energy $E(f)$ for the minimizing interpolant can be calculated as:

$$E(f) = \mathbf{W}_x \mathbf{K} \mathbf{W}_x^T + \mathbf{W}_y \mathbf{K} \mathbf{W}_y^T \tag{9}$$

Figure 1(c) shows the warped version of image 1, i.e. $I_1 \circ f$ and figure 1(d) shows a superposition of the warped image 1 over the original image 2, i.e. $\frac{1}{2}((I_1 \circ f) + I_2)$. The latter shows that f correctly interpolates the non-linear deformation since we can observe that the ridge structures of both images coincide to a large extent.

For the sake of comparison, figure 1(e) shows the kind of result that is obtained if f is restricted to be a rigid deformation plus scaling. In this case the rigid transform f was computed in such a way that it respects the correspondence between two special singularities that can be extracted with high reliability by automatic methods, namely the *core* point (ridge ending in the center of the ridge structure) and the *delta* point (large-scale bifurcation point in the lower-left corner).As it can be observed in figure 1(e), enforcing the correspondence between these two points results in large errors in the position of minutia which are far away from the core or the delta. In addition we can observe how the ridge structures interfere with each other in the superposed image. This illustrates the need for an elastic deformation model, as well as the validity of the proposed thin-plate spline model.

3. Elastic matching with uncertain point-correspondences.

As a first step towards the real problem (where point correspondences are unknown), we shall consider here the problem of *uncertain* point correspondences. Hence, rather than minimizing the deformation energy (2) under the interpolating restriction (1), we shall minimize the combined energy:

$$\tilde{E}_{TPS}(f) = E_{TPS}(f) + \lambda \sum_{i=1}^N \frac{\|f(p_i) - p_i'\|^2}{h_i} \tag{10}$$

(a) Image 1

(b) Image 2

(c) Thin-plate warp with known correspondences

(d) Thin-plate warp with known correspondences

(e) Linear warp

(f) Thin-plate warp with uncertain correspondences

(g) Thin-plate warp with unknown correspondences

(h) Thin-plate warp with unknown correspondences, 30% false negatives and 4% false positives
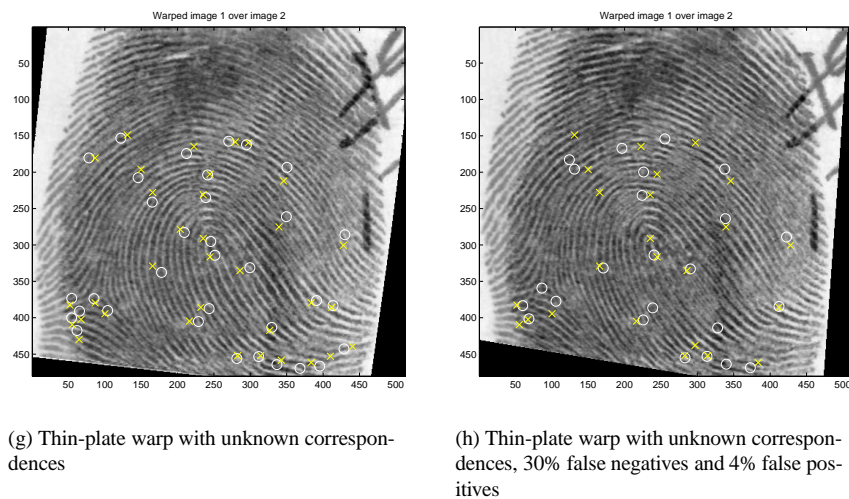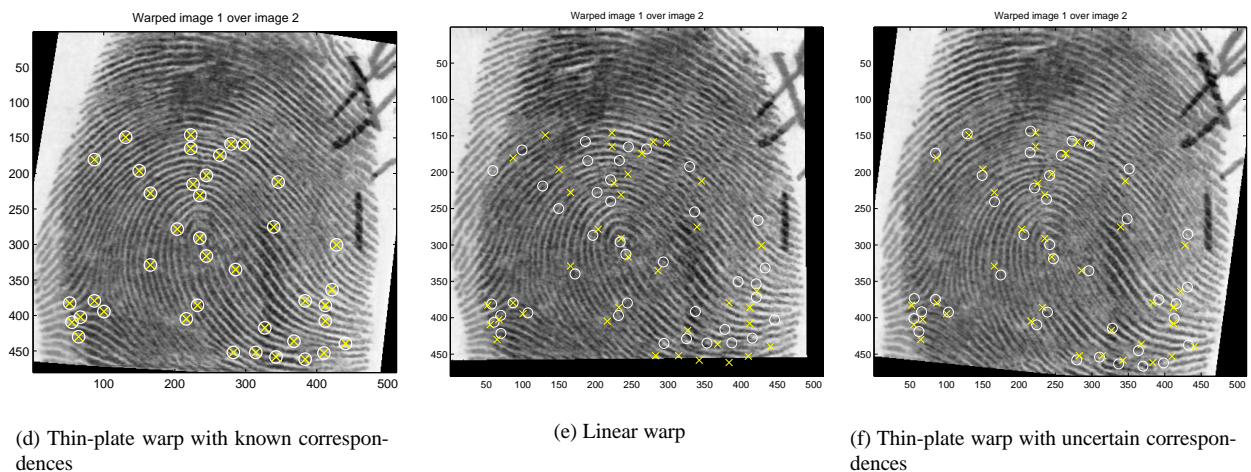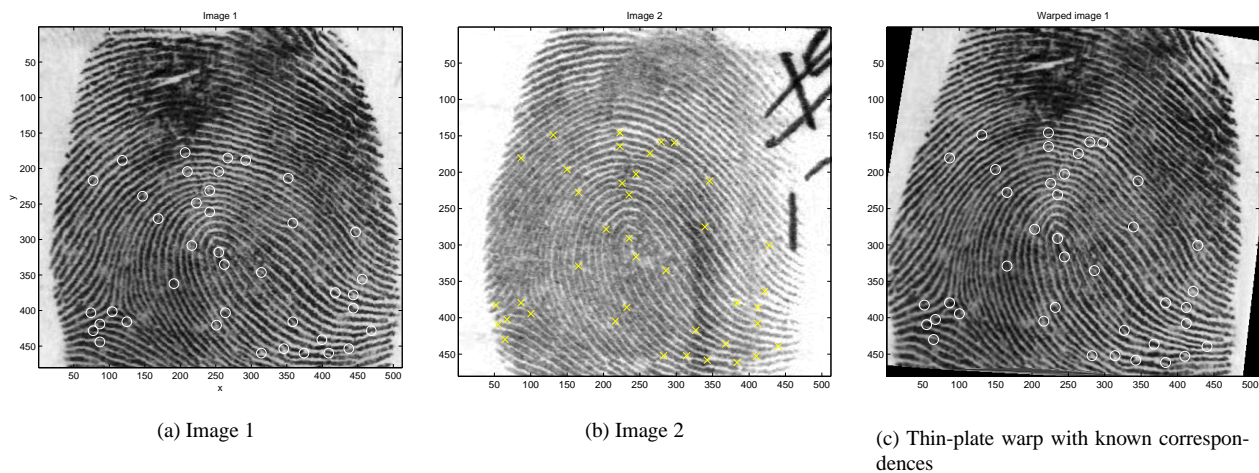
Figure 1. (a-b) Original images and their corresponding minutiae. (c) Image 1 warped by means of a thin-plate spline, in such a way that minutiae coincide. (d) Superposition of the previous warped image 1, with the original image 2. (e-h) Superposition of warped image 1 over image 2 for different warps: (e) Rigid transform plus scaling, chosen to make core and delta points coincide; (f) Thin plate spline, with relaxed interpolation restriction; (g) thin plate spline with unknown point correspondences; (f) thin plate spline with unknown point correspondences, false positives and false negatives.

where λ is a certain Lagrange multiplier and h_i is a measure of the uncertainty of the point correspondence (p_i, p'_i).

Then, according to [15], the solution can be obtained in the same manner as in the previous section, but replacing the matrix K by $\tilde{K} = K + \frac{16\pi}{\lambda} \text{diag}(h)$, and the resulting minimal deformation energy becomes

$$\tilde{E}_{TPS}(f) = 16\pi(\mathbf{W}_x \tilde{\mathbf{K}} \mathbf{W}_x^T + \mathbf{W}_y \tilde{\mathbf{K}} \mathbf{W}_y^T) \quad (11)$$
$$+\lambda \sum_{i=1}^{N} \frac{\|f(p_i)-p'_i\|^2}{h_i}$$

In the absence of any information on the reliability of point correspondences we set $h_i = 1$ for all i. Figure 1(f) shows the warp f that is obtained by minimizing (10) for $\lambda = 10^{-5}$. As it can be seen the result is more or less "halfway" between the minimizer of E_{TPS} and the rigid transformation. The largest errors occur in those regions where the image is most deformed or the points were incorrectly positioned by the operator. Observe for instance the two points near the core of the image. In image 1 they are much far away than in image 2. While decreasing the first term of the energy, an exact correspondence of these points would highly increase the deformation energy.

4. Elastic matching with unknown point-correspondences.

In general we do not know the exact point correspondences. We only have a sequence $p = (p_1, p_2, \ldots, p_N)$ of minutiae in the first image, and a sequence $p' = (p'_1, p'_2, \ldots, p'_M)$ of minutiae in the second image. In such a situation, we can search for a deformation function f of minimal deformation energy (regularization term), such that the distance between $f(p)$ and p' is minimal (data fitting term), i.e. we shall minimize:

$$E(f) = E_{TPS}(f) + \lambda \sum_{i=1}^{N} P(f(p_i)) \quad (12)$$

$$P(a) = g(\inf_{j=1,\ldots,M} \|a - p'_j\|) \quad (13)$$

The data-fitting potential P is a function g of the distance from the deformed point $a = f(p_i)$ to the closest data point p'_j. For simplicity we used here $g(d) = \frac{\alpha}{2}d^2$, but we may consider e.g. the more robust $g(d) = \inf(\beta, \frac{\alpha}{2}d^2)$ in order to reduce the effect of outliers, and reduce the computation time as well (since operations become more local).

Before we explain how the minimization of (12) is solved, let us first show some results. In a first simple case (see figure 1(g)), we assume there are no false positives and no false negatives. Both sequences p and p' only contain true information, but the algorithm has to find the correspondences (p_i, p'_{j_i}).
This correspondence is considered to be given by the arg inf

in equation (13). In fact, if $P(f(p_i)) = g(\|f(p_i) - p'_{j_i}\|)$ (i.e. if p'_{j_i} is the closest data point to $f(p_i)$), then we consider that the match (p_i, p'_{j_i}) was found by the algorithm. In this example it turns out that minimization of (12) by the method that will be explained in the next section, yields only 1 incorrect match among the 34 available pairs, whereas the rigid transformation shown in figure 1(e) yields 6 incorrect matchings.

As a second example we consider a more realistic situation, where we removed 30% of the minutiae of each image independently (i.e. 11 out of 34), and added 4% of false minutiae in each image (i.e. 1 minutia). This leaves 17 correct pairs of minutia in common, i.e. only half of the pairs. The resulting transformation is shown in figure 1(h). In this case 15 out of the 17 available pairs were matched correctly, but we observe a total of 9 false matches: 2 incorrectly matched pairs, 2 false matches due to the false minutiae, and 5 false matches due to the fact that a match is enforced even for those minutiae of image 1 which do not have a corresponding minutia in image 2. In section 6 we propose several ways to improve this preformance.

5. Two-step iterative algorithm.

The energy to be minimized in equation (12) may be non-convex and extremely complex. Hence, we shall solve the optimization problem, by means of an iterative two-step algorithm, where each step is a convex and much simpler to solve optimization problem.

Let $u = p'$ be the minutiae to be fitted in image 2, and p the minutiae in image 1. The purpose is to find a function f with low deformation energy, such that each transformed minutia from image 1 $v_i = f(p_i)$ lies close to some minutia u_{j_i} in image 2. Let us rewrite equation (12) in terms of u and v as $E(v) = E_{TPS}(v) + \lambda \sum_i P(v_i)$ where the data-fitting potential P depends on $u = p'$ as defined in equation (13); and $E_{TPS}(v) = E_{TPS}(f^{p,v})$ as defined in (12) being $f^{p,v}$ the thin-plate spline interpolant such that $f(p) = v$.

We now introduce an auxiliary variable w as follows:

$$E_{\text{aux}}(v, w) = E_{TPS}(v) + \frac{\lambda}{2} \sum_i \|v_i - w_i\|^2 \quad (14)$$
$$+ \lambda \sum_i P_1(w_i)$$

Then, as shown in [8] minimizing $E(v)$ is equivalent to minimizing E_{aux} first on w and then on v, and both minimization problems become convex, provided P_1 can be properly chosen. In our case, since $P(a) = g(d(a, u))$ is defined as a certain function g of the distance to the data points u, it suffices to define $P_1(a) = g_1(d(a, u))$, where g_1 can under certain hypothesis be expressed in terms of

the conjugate function of $(\frac{x^2}{2} - g(x))$, which in our case becomes $g_1(d) = \frac{\alpha}{\alpha-1}\frac{d^2}{2}$.

The alternate minimization property described above justifies the following two-step algorithm:

0. *Initialization.* $w^0 = v^0 = T(p)$, $n = 0$. Here T is a rigid transformation plus a scaling which maps the corresponding core and delta points as explained at the end of section 2, and in figure 1(e).

1. *Data fitting:* $w^{n+1} = \arg\inf_w E_{\mathrm{aux}}(v^n, w)$

2. *Regularization:* $v^{n+1} = \arg\inf_v E_{\mathrm{aux}}(v, w^{n+1})$

3. Iterate steps 1 and 2, incrementing n until convergence.

Since the first term of E_{aux} does not depend on w, the minimization in step 1 is equivalent to minimizing over w:

$$E_1(v, w) = \sum_i \left(\frac{1}{2}\|v_i - w_i\|^2 + P_1(w_i) \right) \qquad (15)$$

which is easy to solve, since it is piecewise quadratic on w, with one piece for each Voronoi cell of the set of points u. Hence, a very efficient algorithm can be written.
Similarly, since the last term of E_{aux} does not depend on v, the minimization in step 2 is equivalent to minimizing over v:

$$E_2(v, w) = E_{TPS}(v) + \frac{\lambda}{2}\sum_i \|v_i - w_i\|^2 \qquad (16)$$

which is exactly the problem we solved in section 3.

Over the iterations we observe that very often false matches found in step 1, are corrected in the next iteration, thanks to the regularization in step 2. After a certain amount of iterations (usually less than 10 in our experiments) the process converges to a stable matching, and consequently v remains stable. False matchings remaining in this final state, most often confuse minutiae which are very close to each other, which permits to keep the false match without incrementing too much the deformation energy. In this example the number of false matches decreases from 6 in the first iteration, to 3 in the third iteration, 2 in the fifth and 1 after the seventh iteration.

6. Summary and Discussion.

In this work we showed the suitability of the thin-plate spline model as a way to represent the kind of deformations that can be observed between different samples of the same fingerprint. In addition, we showed how such a deformation model can be effectively used, in order to improve the performance of fingerprint matching algorithms, most often based on rigid transformations.

Since this is only possible at the cost of a computationally more expensive procedure, the proposed method is only intended as a last-stage precise matching algorithm, that may be used to safely reduce a candidate list previously generated by other algorithms which impose simpler geometric constraints.

Even though the proposed algorithm performs well in the absence of noisy data, in a realistic situation (where there is a large number of false positives and false negatives) the estimated deformation is still far from the correct one, but still better than a rigid transformation. In order to improve this performance many complementary directions can be followed:

Adapting the data fitting potential P to ensure a one-to-one partial mapping between u and v. The main difficulty may be related to the existence of the corresponding potential P_1, to be used in the two-step iterative algorithm.

Using a richer feature space to avoid incorrect minutia pairings. In addition to the spatial position currently used, feature detection algorithms can produce more information like *ridge orientation*, *curvature*, *width*, *minutia type*, *ridge count* between pairs of minutiae, *local image quality*, etc.

Weighted matching. The weight h_i introduced in equation (10) can be chosen as a function of local image quality as proposed by [12]. These authors obtained significant improvements with respect to the non-weighted version, but did not include an elastic deformation model.

Incremental processing. Instead of treating all minutiae at once, we can accept point matches and compute the deformation in an incremental manner, by processing the data points in a spiral fashion around the core point, as proposed in [13, 11]. Thus they exploit the higher reliability of the correspondence between core points. Consequently each accepted match is most likely sure, and no extra-iterations are needed to undo false matches.

References

[1] A. Almansa and T. Lindeberg. Fingerprint enhancement by shape adaptation of scale-space operators with automatic scale selection. Technical report, Dept. of Numerical Analysis and Computing Science, KTH, Jan. 1999. http://www.nada.kth.se/abstracts/cvap226.html.

[2] N. Arad, N. Dyn, D. Reisfeld, and Y. Yeshorun. Image warping by radial basis functions: Application to facial expressions. *Computer Vision, Graphics, and Image Processing : Graphical Models and Image Processing*, 56(2):161–172, Mar. 1994.

[3] K. Asai, Y. Hoshino, N. Yamashita, and S. Hiratsuka. Fingerprint identification system. In *Second USA-Japan Computer Conference*, pages 30–35, 1975.

[4] O. Bergengruen. Matching of fingerprint images. Technical report, Dept. of Numerical Analysis (CeCal), School of

Engineering, University of the Republic of Uruguay, Montevideo, 1994.

[5] F. L. Bookstein. Principal warps: Thin plate splines and the decomposition of deformations. *IEEE Trans. Pattern Analysis and Machine Intell.*, 11(6):567–585, June 1989.

[6] R. J. Castro-Latorre. Manual de dactiloscopía. Dirección Nacional de Identificación Civil, Ministerio del Interior, Uruguay, 1993.

[7] W. W. Clements. *The Study of Latent Fingerprints. A Science*. Charles C. Thomas - Publisher, Springfield, Illinois, USA, 1987.

[8] L. D. Cohen. Auxiliary variables and two-step iterative algorithms in computer vision problems. *J. of Mathematical Imaging and Vision*, (6):59–83, 1996.

[9] DNPT. Manual de dactiloscopia. Ministerio del Interior, Uruguay.

[10] FBI. The science of fingerprints. classification and uses. U.S. Department of Justice, FBI. Superintendent of Documents, U.S. Government Printing Office, Washington, D.C. 20402. Stock Number 027-001-00033-5 / Catalog No. J1.14/2:F49/12/977, 1984.

[11] A. Jain, L. Hong, and R. Bolle. On-line fingerprint verification. *IEEE Trans. Pattern Analysis and Machine Intell.*, 19(4):302–3013, Apr. 1997.

[12] F. R. Johannesen, S. Raaschou, O. V. Larsen, and P. Jürgensen. Using weighted minutiae for fingerprint identification. In *Advances in Structural and Syntactical Pattern Recognition. 6th International Workshop, SSPR '96 Proc.*, pages 289–99. Springer-Verlag, 1996.

[13] Karu and Jain. Fingerprint classification. *Pattern Recognition*, 1996.

[14] Kim, Kim, and Sakata. Automatic fingerprint verification system. In *Proc. TECON*, 1987.

[15] B. Leroy. *Modèles Déformables et Modèles de Déformation Appliqués à la reconnaissance de visage*. PhD thesis, Université Paris-IX Dauphine, 1996.

[16] B. Leroy, I. L. Herlin, and L. D. Cohen. Face identification by deformation measure. In *Proc. 13th International Conference on Pattern Recognition*, Vienna, Austria, 1996. IEEE Computer Society Press.

[17] D. Maio and D. Maltoni. Direct gray-scale minutiae detection in fingerprints. *IEEE Trans. Pattern Analysis and Machine Intell.*, 19(1):27–40, Jan. 1997.

[18] Mital, Kwang-Teoh, and Amarasinghe. An automated matching technique for identification of fingerprints. In *Proc. SPIE*, volume 2908, 1996.